Title

Oxidative Dehydrogenation of Cyclohexane by Cu *vs* Pd Clusters: Selectivity Control by Specific Cluster Dynamics

Journal

ChemCatChem, 12(5)

ISSN

1867-3880

Authors

Halder, Avik
Ha, Mai-Anh
Zhai, Huanchen
et al.

Publication Date

2020-03-06

DOI

10.1002/cctc.201901795

Peer reviewed

Oxidative Dehydrogenation of Cyclohexane by Cu *vs* Pd Clusters: Selectivity Control by Specific Cluster Dynamics

Avik Halder,[1€] Mai-Anh Ha,[2€] Huanchen Zhai,[2] Bing Yang,[1] Michael J. Pellin,[1] Sönke Seifert,[3] Anastassia N. Alexandrova,[2,4]* Stefan Vajda,[1,5,6]*

[1]*Materials Science Division, Argonne National Laboratory. 9700 South Cass Avenue. Lemont, Illinois 60439, USA*
[2]*Department of Chemistry and Biochemistry, University of California, Los Angeles, Los Angeles, California 90095, USA*
[3]*X-ray Science Division, Argonne National Laboratory. 9700 South Cass Avenue. Lemont, Illinois 60439, USA*
[4] *California NanoSystems Institute, Los Angeles, California 90095, USA*
[5] *Institute for Molecular Engineering, The University of Chicago, 5640 South Ellis Avenue, Chicago, Illinois 60637, USA*
[6] *Department of Nanocatalysis, J. Heyrovský Institute of Physical Chemistry, Czech Academy of Sciences, Dolejškova 3, 18223 Prague 8, Czech Republic*

[€]Authors contributed equally
*Corresponding Authors' emails: ana@chem.ucla.edu, stefan.vajda@jh-inst.cas.cz

ABSTRACT

Supported subnanometer clusters can exhibit precious catalytic properties not observed in their bulk analogues. Partially-oxidized Pd and Cu clusters are reported to catalyze the oxidative dehydrogenation of cyclohexane with high activity, and with distinctly different selectivity, producing primarily benzene or cyclohexene, respectively. Under reaction conditions, the structure and oxidation state of the two catalysts evolve differently which leads to either the desorption of the cyclohexene intermediate or to its deeper dehydrogenation. Under the applied reaction conditions the initially oxidized Pd and Cu clusters undergo partial reduction, which we show to be required for the selectivity to emerge. Both systems also have thermal access to multiple distinct structural forms yielding statistical ensembles. The structures within these ensembles evolve with the changing nature of the bound reaction intermediates differently for the two metals; the evolution is found pronounced in the Cu clusters, but only modest in Pd. Ultimately, the different selectivity observed experimentally for the Cu versus Pd clusters is controlled by differences in the collective structural and redox dynamics of their ensembles.

Introduction

Small supported clusters are unique and puzzling catalysts: their properties are strongly size-, composition-, and support-sensitive.[1-10] Recently, we have noted that such catalysts present a variety of structures that easily interconvert at catalytic temperatures, thus collectively defining the properties of the catalyst.[10-17] Here, we present a set of subnanometer Pd and Cu cluster catalysts that exhibit very different and highly competitive selectivities for oxidative dehydrogenation (ODH) of cyclohexane.[2,18-23] We show that the observed differences in the catalysts' performance are ultimately linked to both structural and redox evolution within the evolving ensembles of thermally accessible catalyst states under applied reaction conditions.

The desirable products obtained by the oxidative dehydrogenation (ODH) of cyclohexane are the partially dehydrogenated intermediates, such as cyclohexene (precursor of adipic acid),[24] cyclohexadiene (precursor for poly-additions[25] and synthetic reagent[26]), and cyclohexanone (precursor of widely used synthetic polymer, Nylon-6,[27] and primary component of Keton-Aldehyde Oil).[28] These occur before the formation of benzene, the possible final C6 product, and CO/CO_2, the undesired combustion products. Despite substantial effort, the selectivity and efficiency of ODH, particularly toward valuable intermediates, remain limited.

Apart from the sub-nano regime, nanoscopic Pd-based catalysts are known to convert cyclohexane to benzene with high selectivity at temperatures around 200ºC.[29] This finding provided a motivation to look at ultrasmall Pd clusters, where the per total atom activity (turn-over frequency, TOF) could potentially be increased as well. Cu presents a potential alternative to Pd, as it was reported that Cu installed in zeolites is capable of producing cyclohexene, methyl cyclopentane and benzene from cyclohexane.[30] Moreover, it was shown that the performance of Cu_xO_y- based catalysts can be tuned for benzene and cyclohexene by changing the structure of the catalyst and the morphology of the support.[31] In this study we focus on the catalytic activity and selectivity of a set of catalyst made of supported subnanometer Cu and Pd clusters in the ODH of cyclohexane.

Results and Discussion

Experimental Section

The catalysts were prepared by depositing size-selected, originally metallic, ligand-free Pd and Cu clusters from the gas phase[32] on alumina, titania, or ultrananocrystalline diamond (UNCD) support, with the goal to explore the effect of cluster size and the nature of the support on catalytic activity and selectivity.[1,3] The catalysts were tested and characterized using a multiprobe *in situ* approach that combined temperature programmed reaction (TPRx), grazing incidence X-ray absorption spectroscopy (GIXAS), and grazing incidence small-angle X-ray scattering (GISAXS), to find a correlation between catalytic performance and the oxidation state of the metal under realistic reaction conditions of temperature and pressure, while also allowing simultaneous monitoring of the sintering resistance of the clusters.[3,6,32] Further details on the experimental methods are given in in Experimental Methods section and in the Supporting Information (SI).

Catalytic performance. The performance of the Pd cluster-based catalysts is shown in **Figure 1**. , with the applied temperature ramp shown in **Figure 1a.** Pd clusters of all sizes and on all supports produce benzene and CO_2 with minute amounts of cyclohexene. The rates of product formation (*r – per total atom activity, TOF*) were determined as the number of product molecules produced per metal atom per second (mol/at/s). In **Figure 1b,c**, we show *r* for benzene and CO_2 on supported Pd_4 clusters at 300ºC (for the Pd_5 and Pd_8 clusters please see the Supplemental Information). On all supports, the selectivity of the reaction towards benzene, when catalyzed by the Pd tetramers, increases as the temperature grows from 200ºC to 300ºC (**Figure 1d**), contrary to the temperature-dependent performance reported for larger Pd nanoparticles.[29] At 300ºC, with *r* for benzene produced by Pd clusters of various sizes supported on UNCD, the activity ranks as Pd_4>Pd_5>Pd_8. Pd_4 is the most interesting cluster size with a maximum *r* of 0.49 mol/at/s for benzene, which is significantly higher than some of the best reported for the bulkier catalyst (**Table S1**).[21,29,31,33-38] Unexpectedly, at 300ºC there is no strong dependency in the formation rate of benzene on the Pd cluster size with a given oxide support: *r* is ~0.25 on alumina and ~0.18 mol/at/sec on titania (**Figure S2**). However, the carbon-based selectivity toward benzene at 300ºC exhibits a strong cluster size dependency: for Pd_4 and Pd_5 on UNCD *r* is ~40%, for Pd_8 on UNCD it is ~30%, while it is ~20% and ~15% for all cluster sizes on Al_2O_3 and TiO_2 support, respectively.. The rate of CO_2 formation on the oxide-supported Pd clusters is almost the double of that of UNCD-supported ones (**Figure S2, S3**). Hence, the support effect offers a possible control knob to tune the selectivity in this reaction. In addition to benzene, about 10-15% of cyclohexene was also detected, most notably on titania at lower temperatures, before dropping to ~ 5% at 300 ºC. The reproducible activity during the heating and cooling cycle indicates that the catalysts do not deactivate during the applied temperature ramp nor sinter as indicated by GISAXS (**Figure S4**).

The oxidation state of Pd in the Pd_4/UNCD catalyst evolves with temperature during the applied temperature ramp as shown in **Figure 1f**. At the start of the ramp (150-250ºC), Pd has the average oxidation state of +2. At 300ºC, the highest temperature applied, the average oxidation state of Pd in Pd_4 clusters is found to be the highest on the UNCD support(~ +1.2) and the lowest on the titania support (~ +0.8) as shown in **Figures S5-S7**. During the cool-down phase of the applied temperature ramp, a partial reoxidization of Pd is observed. Therefore, theoretical calculations will focus on Pd_4O_2/UNCD, representing the average oxidation state of Pd^{+1} at conditions of the highest selectivity for benzene.

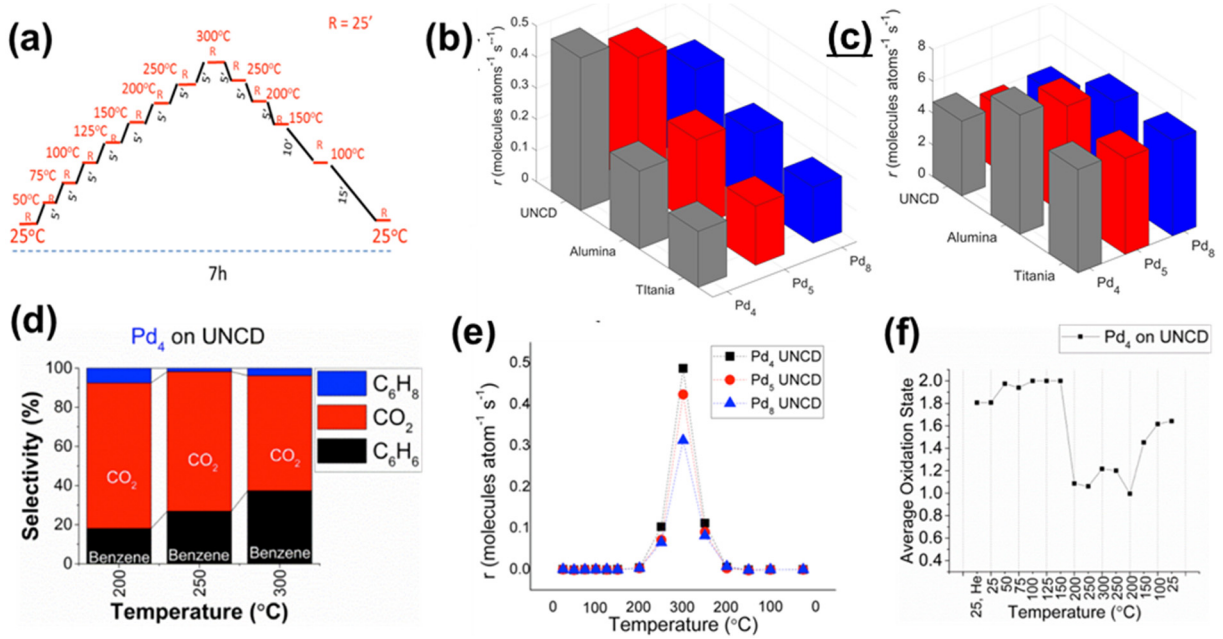

Figure 1: (a) Temperature ramp applied, with R denoting the time (25 minutes) the temperature was kept at each temperature step. Plots of per total Pd atom *r* for benzene (b) and CO_2 (c) at 300ºC for Pd_n (n=4,5,8) on UNCD, Al_2O_3, and TiO_2 supports. (d) Selectivity towards the products benzene, cyclohexene, and CO_2 plotted for Pd_4 on UNCD. (e) Evolution of the reaction rate *r* for benzene during the temperature ramp for Pd_n(n=4,5,8) clusters supported on UNCD. (f) Evolution of the average oxidation state of Pd in Pd_4 clusters supported on UNCD, obtained from the linear combination fit (LCF) analysis of the *in situ* Pd K-edge XANES spectra (estimated uncertainty ± 0.1). The reactant mixture used was 0.4 % cyclohexane (4000 ppm in helium) and 4 % O_2 (99.999% purity) seeded in He, fed to the reaction cell at a flow rate of 20 sccm. The pressure inside the reactor cell was maintained at 1.1 atm.

Motivated by the high activity and selectivity of UNCD-supported Pd_4 and Pd_5 clusters for benzene formation, we next investigated the UNCD-supported Cu_5 clusters under identical reaction conditions. **Figure 2** shows the experimental results obtained on the Cu_5/UNCD catalysts: First, the activity of the Cu_5 clusters is found to be significantly higher than that of the Pd clusters (**Figures 2a, S6**), with a cumulative activity *r* for all C6 products of ~2.5 molecules atom^{-1} s^{-1}, which is about 5 times higher than the overall rate of C6 formation on Pd clusters on the same support (~0.5 mol/atom/s). Moreover, at 300°C, the Cu_5 clusters exhibit much higher selectivity, up to about 30%,towards the C6 products (**Figure 2b**). In contrast to Pd, Cu_5 produces only a small fraction of benzene (4%) along the much more dominant cyclohexene (34%) and cyclohexadiene (8%). A very small fraction (1%) of cycloxenanone was also detected.

The oxidation state of Cu during the applied temperature ramp evolves with temperatures as shown in **Figures 2c and S7**. At lower temperatures, the average oxidation state of Cu is close to +2. Above 200ºC, a partial reduction of Cu is observed, leading to an average oxidation state of +1.7 at 300ºC. During the cool down phase the clusters fully reoxidize, in contrast to the Pd clusters. The fully reversible redox behavior of copper suggests a higher chemical flexibility in the Cu clusters i.e. a lack of kinetic hindrance toward accepting or releasing oxygen in comparison with palladium. The fact that the appearance of the most

reduced state of copper correlates with the highest selectivity toward cyclohexene formation, hints to the potential importance of a partially reduced state in the formation of cyclohexene. GISAXS showed no evidence for agglomeration of Cu clusters on UNCD, confirmed by the unchanged GISAXS patterns collected during the applied temperature ramp. (**Figure S8**).

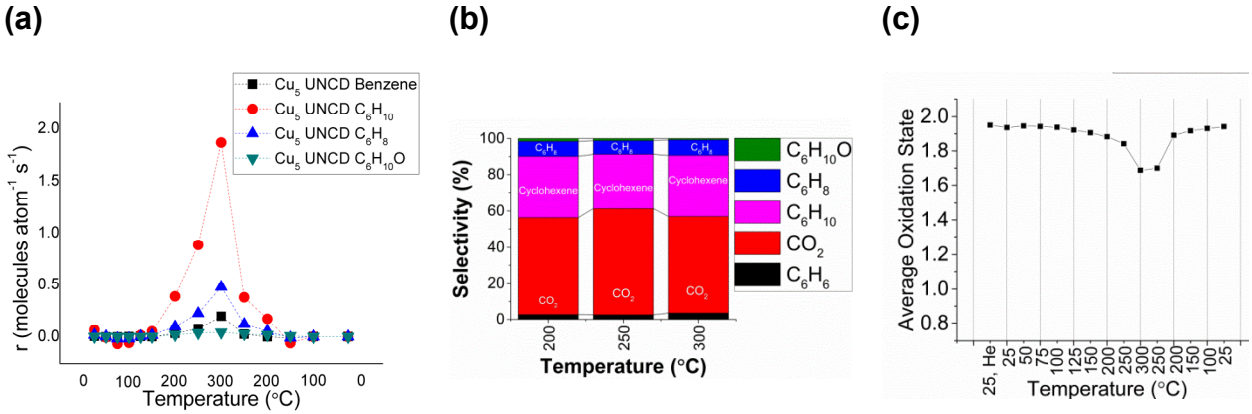

Figure 2. Cu_5 clusters supported on UNCD. (a) Plot of per total Cu atom *r* of benzene, cyclohexene, cyclohexadiene, cyclohexanone, and CO_2 formed. (b) Plot of carbon-based selectivity. (c) Evolution of the average oxidation state of Cu in in Cu_5 clusters obtained from linear combination fit (LCF) of the *in situ* Cu K-edge XANES data collected during the temperature ramp using the spectra of bulk Cu standards shown in FigureS2b. Typical fits are shown in Figure S6. An uncertainty of ± 0.1 is estimated for the average oxidation state calculated.

Computational Section

We sought to determine the origin of the differences in the selectivity of Pd and Cu cluster catalysts using plane-wave density functional theory (PW-DFT). In what follows, Pd-O clusters refer to Pd_4O_2, corresponding to the $Pd^{+1.2}$ oxidation state seen in the experimental *in-situ* XANES (see **Figures S5-S7)** at the highest temperature (300°C) and onset of activity. In view of the specific and fully reversible redox activity of Cu, we explored both the major Cu^{2+} oxidation state (Cu_5O_5) and the minor $Cu^{+1.7}$ oxidation state (Cu_5O_3) that rises at the onset of special activity and selectivity. Note that in the experiment the average oxidation state of the metal might change depending on the bound adsorbate (reactant or reaction intermediate), providing an additional complication in choosing the relevant chemical composition of the cluster for modeling. As shown in Tables S2-S9 in the SI, we find computationally that in fact the average charge on the Pd/Cu atoms within the cluster remains nearly unchanged as a function of the presence and nature of the considered adsorbates. Therefore, we assume that the XANES signal can be mapped on the oxygen content throughout the considered steps of the reaction.

Our goal is to explore the ensemble of all accessible states of the system without and with adsorbates. Ideally, we would want to connect all the found catalysts states with computed reaction barriers, which would constitute around $>10^2$ per state. Clearly, this task in its entirety is computationally unfeasible, requiring calculations including all the permutations of C-C and C-H bond breaking in the forward and reverse reactions. Chen et. al. have demonstrated the difficulty of this task for even the simpler system of ethane on a metal surface, which required

an exhaustive 58 reaction barriers.[39] For this reason, we focus our exploration on just a few key points to capture the signs of selectivity. Since the major difference in selectivity is the production of benzene on Pd and the particularly desirable cyclohexene on Cu, the cyclohexene intermediate appears to be the key species in the reaction, which should either desorb (on Cu), or continue undergoing ODH (of Pd). Therefore, we focus our calculations on three states along the reaction profile: the state of the partially oxidized catalysts that would form *in situ* but without C6 adsorbates, the catalysts with adsorbed cyclohexane (reactant), and the catalysts with cyclohexene (selectivity-determining intermediate). At the step with cyclohexene, an important bifurcation takes place: it more easily desorbs from Cu, but continues undergoing ODH on Pd.

Using PW-DFT, we performed global optimizations and considered ensembles of all thermally-accessible minima of the supported clusters as a function of adsorbed reagents at the high temperature limit of 573 K (300°C). In **Figure 3**, the lowest-energy minima of UNCD-supported Pd_4O_2, both adsorbate-free and with adsorbates, are shown. For every minimum, we compute the temperature-dependent Boltzmann probabilities to be present in the ensemble, P_{535K} (more minima and data included in **Figures S11,S12, Tables S2-S4)**. This approach operates under the assumption that all low-energy isomers are kinetically-accessible and thus can be populated according to the simple Boltzmann statistics. In fact, it is not known whether or not all minima are kinetically-accessible and confirming this would be an intractable task. However, in one exhaustive study we showed that at least for Pt clusters on α-alumina, the cluster isomerization is highly facile, and all of ~30 low-energy minima are indeed easily visited by the system in under 1 ns.[12] Furthermore, since we introduced the Boltzmann ensemble approach, we successfully used it to describe a number of cluster catalyst properties, such as sintering on the support,[16,17] size-specific catalytic activity,[10] and composition-dependent selectivity,[11,13,15] in agreement with experiment when it was available.[10,11,16] In the case of Pd on UNCD, we note that the global minimum may constitute only circa 43-46% of the population, depending on the reaction step (see Figure 3, ~43% for global minimum of adsorbed C_6H_{12}; ~46% for adsorbed C_6H_{10}). Therefore, the global minimum alone cannot accurately represent the catalyst. Less stable isomers are likely to be more chemically reactive and therefore cannot be ignored.[6,10,11,13,1540,41] In **Table 1**, we specify the number of thermally-relevant isomers of supported clusters and the average charges on the metal atoms. The Pd atoms within the Pd_4O_2 clusters are charged non-uniformly: the topmost Pd have a small negative charge, while the Pd connected to oxygen or carbon report a small positive charge. Note that the charge is far from the formal oxidation state, which is not unusual. DFT tends to over-delocalize electrons in solids and the multicentered interactions of coordinated bonds further complicate charge interactions so that most charge partitioning schemes, including Bader, cannot differentiate *shared* charge density.[42] This is a known deficiency in the Bader charge calculation algorithm, but these partial charges remain of interest in clarifying surface chemical processes by describing relative charges to atomic charges.[43] We note that this deficiency will be even more exaggerated in supported clusters where metal-support interactions are more diffuse than the stronger metal-ligand interactions within a crystalline solid.

In all identified isomers, the Pd core in the cluster is generally tetrahedral and remains remarkably insensitive to the lack or presence of the adsorbates (**Figure 3**). Note that in the clusters without the C6 adsorbates, the global minimum is exceptionally dominant and constitutes ~98% of the population. Upon the adsorption of cyclohexane, the population

becomes more diverse with several states showing significant populations. However, the isomers of the reagent-adsorbed state differ only by the adsorption site and the Pd_4O_2 catalyst remains unchanged with Pd-Pd bonds remaining an average of 2.6 Å and Pd-O bonds, an average of 2.2 Å (see SI Table S2-S4 for bond lengths without and with adsorbates). The lowest-energy structures of adsorbed cyclohexane feature the Pd-H contact of circa 2.0-2.2 Å, initiating the C-H bond activation toward dehydrogenation. Cyclohexene binding causes somewhat greater changes for the clusters. In certain configurations, the Pd-O bond (minima iii, v, vi in **Figures 3** and **S11, S12**) or Pd-Pd bond (minimum viii in **Figure S12**) is broken to accommodate the adsorption of cyclohexene. In all the isomers, cyclohexene is bound to Pd via the double C-C bond (the Pd-C bond is an average of ~2.2 Å, see Table S4) either at the topmost Pd (isomers i, vii, viii) or to one of the basal Pt (isomers ii-vi). Pd_4O_2, in response to the adsorbed cyclohexene, will tilt towards the surface, resulting in Pd coordinating to and transferring a slight charge to a surface hydrogen. Cyclohexane and cyclohexene adsorb to Pd_4O_2 with Boltzmann-weighted adsorption energies ($\Sigma P_{535K}E$) of -0.63 eV and -1.32 eV, respectively. The favorable adsorption of reaction intermediates agree with the high rate of benzene formation observed in experiment.

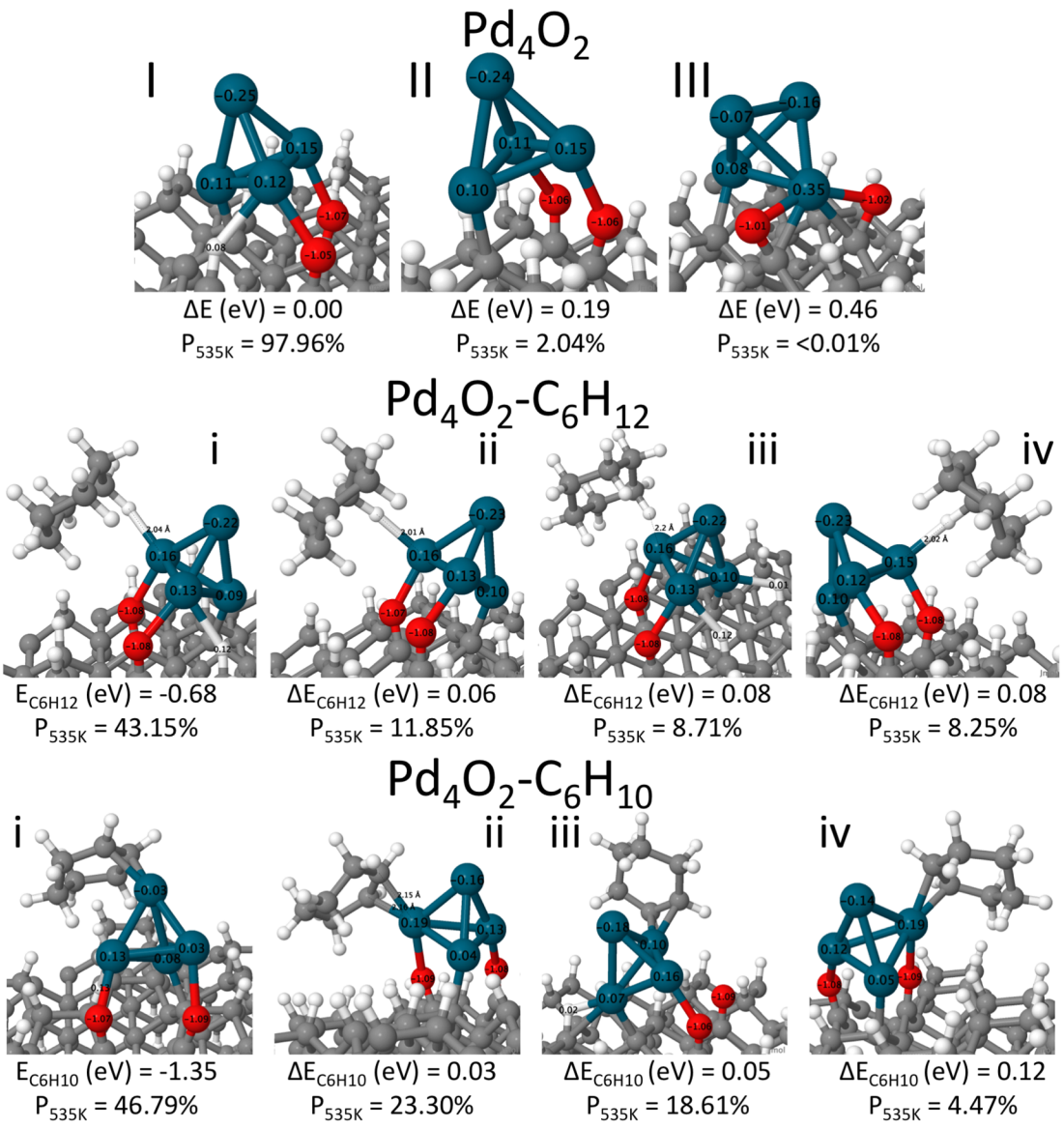

Figure 3: The lowest-energy minima of Pd_4O_2/UNCD adsorbate-free and with C_6H_{12} and C_6H_{10} adsorbed. Adsorption energetics and Boltzmann populations are illustrated below the minima. Further details of all minima considered are in the SI (Tables S2-S4; Figures S10, S11). Carbon atoms are in gray, hydrogen in white, palladium in teal, and oxygen in red. Detailed bonding information such as bond lengths within the cluster and cluster-reagent interactions may be found in the SI Tables S2-S4.

Table 1. Key Reaction Intermediates on Supported Metal-Oxide Clusters: Number of Configurations of Cyclohexane and Cyclohexene, Reaction Energetics (Boltzmann-weighted adsorption energies, $\mathbf{\Sigma P_{535K}E_{react}}$ and Reaction Energy, $\mathbf{\Delta E}$), Average charge of M^+ ($\Delta Q_{M,avg}$).

Adsorbed Reactants	**# Isomers.**	$\mathbf{\Sigma P_{535K}E_{react}}$ **(eV)**	$\mathbf{\Delta Q_{M,avg}}$ **(e)**
Pd_4O_2	3		0.04
Pd_4O_2 - C_6H_{12}	12	-0.63	0.03
Pd_4O_2 - C_6H_{10}	8	-1.32	0.04
$\mathbf{\Delta E_{C6H12->C6H10+H2}}$ **(eV)**		0.82	
Cu_5O_5	3		0.46
Cu_5O_5 - C_6H_{12}	23	-0.56	0.53
Cu_5O_5 - C_6H_{10}	8	-1.38	0.53
$\mathbf{\Delta E_{C6H12->C6H10+H2}}$ **(eV)**		0.70	
$\mathbf{\Delta E_{C6H12+1/2O2->C6H10+H2O}}$ **(eV)**		1.34	
Cu_5O_3	3		0.36
Cu_5O_3 - C_6H_{12}	14	-0.57	0.50
Cu_5O_3 - C_6H_{10}	8	-1.07	0.45
$\mathbf{\Delta E_{C6H12->C6H10+H2}}$ **(eV)**		1.01	
$\mathbf{\Delta E_{C6H12+1/2O2->C6H10+H2O}}$ **(eV)**		2.13	

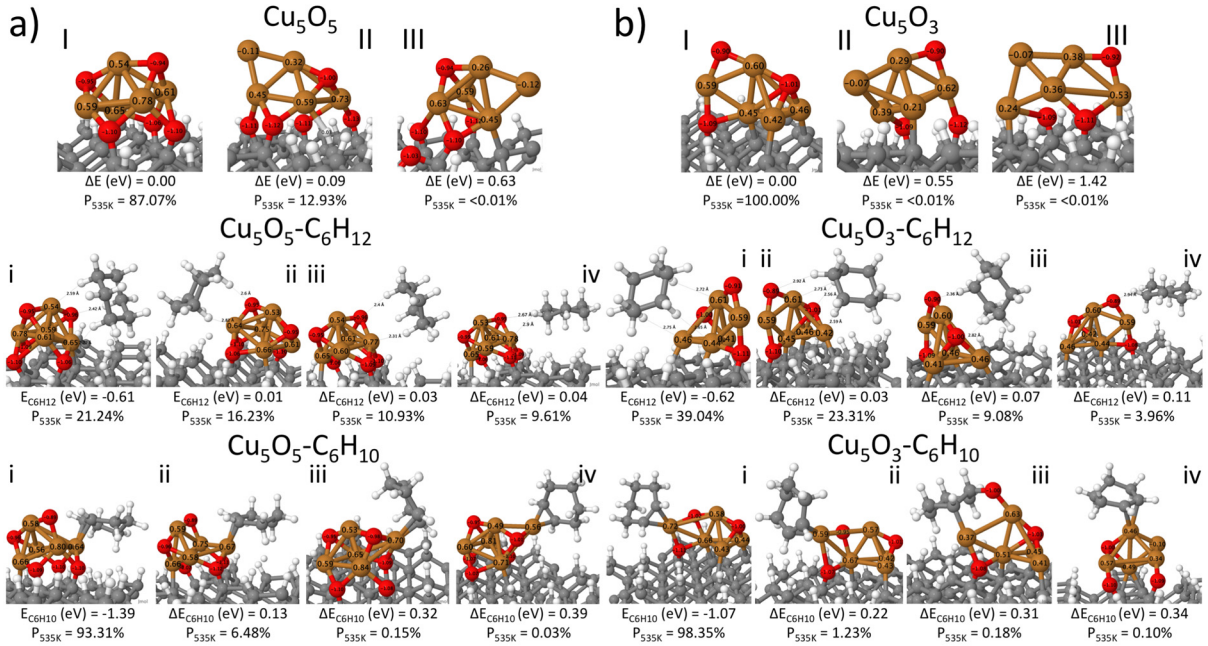

Figure 4: The lowest minima of UNCD-supported (a) Cu_5O_5 and (b) Cu_5O_3, adsorbate-free, and with C_6H_{12} and C_6H_{10} bound. Cu_5O_5 represents the Cu-O catalyst in its as-prepared state and Cu_5O_3, the catalyst under reaction conditions. Adsorption energetics and Boltzmann populations are shown below the structures. Further details of all minima considered are provided in **Tables S5-S10, Figures S13-S16**. Carbon atoms are in gray, hydrogen in white, palladium in teal, and oxygen in red. Detailed bonding information such as bond lengths within the cluster and cluster-reagent interactions may be found in the SI Tables S5-S10.

The results of the calculations for Cu clusters, in both oxidation states, are presented in **Figure 4** and **Table 1** (and **Figures S13-S16**, **Tables S5-S10**, SI). Cu atoms in supported Cu-O clusters exhibit non-uniform computed charges, but are more oxidized as compared to Pd-O, with ΔQ_{Cu} reaching a maximum of +0.8 e. Whereas Pd catalysts remain tetrahedral, Cu catalysts manifest a range of geometries from pseudo-pyramidal to planar "standing" structures with a concomitant diversity in bond-lengths within these structures: Cu-Cu bonds' are 2.3-3.5 Å and Cu-O bonds' are 1.8-2.6 Å (SI Tables S5-S6). In contrast, Pd-Pd and Pd-O bonds differ only by ±0.2 Å; Pd-Pd bonds are also considerably shorter than Cu-Cu bonds reinforcing the compactness of the Pd_4O_2's tetrahedral configuration as compared to $Cu_5O_{n=3,5}$ (SI Table S2). The oxygen atoms are present both at the cluster-support interface and at bridging (coordinated to two Cu atoms) and hollow sites (coordinated to three Cu atoms) of the cluster. Hence, both Cu and O atoms at the surface of cluster are available to interact with reactants (**Figure 4**). Note that all O or Cu atoms in these clusters are unique in term of coordination and charge. Different coordinations at these sites suggest different reactivities. Pd-O and Cu-O clusters (for both oxidation states of Cu) bind cyclohexane similarly, with a favorable adsorption of ~ -0.6 eV and coordination to one or two cyclohexane H atoms.

In contrast with Pd-O, the isomers of Cu_5O_3 and Cu_5O_5 differ not only by the placement of cyclohexane on the cluster, but also by the cluster geometry. Cu-O clusters are more diverse than Pd-O with geometries that resist conventional, prismatic definitions enabling cyclohexane to adsorb weakly in many different configurations. Whereas cyclohexane's hydrogens will more strongly coordinate to Pd atoms with bonds of ~2.0 Å, the hydrogens weakly coordinate

to Cu and O atoms with interactions averaging between circa 2.2-3.0 Å (**SI Table S3, S7, S9**). Since Cu-O clusters feature a greater range in bond lengths and sites (surface Cu and O atoms), this contributes to the diversity of interactions between the cluster and cyclohexane. This may contribute to the large fraction of cluster population spilling out of the global minima to other higher-energy isomers of adsorbed cyclohexane. Whereas the global minimum of adsorbed cyclohexane on Pd_4O_2 contributes to the Boltzmann populations ~ 43%, this drops for Cu-O clusters, particularly, on Cu_5O_5 to ~ 21% and, more moderately, on Cu_5O_3 to ~ 39% (Figures 3-4).

Structural isomerization in general lowers the energy of the system, as it allows the cluster relaxation under the influence of the bound adsorbate. Hence, the greater the structural change —the more stable the reaction intermediate will be. Cu-O and Pd-O clusters with bound adsorbates feature qualitatively different degree of structural diversity. Cu-O clusters are significantly more flexible than Pd-O, and this allows Cu-O clusters binding the reagents with the affinity similar to that of Pd-O. The stabilization through strong catalyst rearrangement is a special feature of very small clusters (or otherwise highly-dynamic interfaces),[44]not accessible to more rigid extended surfaces. One of the consequences of this tendency to strongly rearrange is a routine break down of scaling relations in catalysis.[45] In the present work, structural flexibility, together with the oxidation state change, is linked to catalyst selectivity.

The binding affinity for cyclohexene shows important differences between the studied clusters. Cu_5O_5 binds cyclohexene more strongly than does Pd_4O_2, whereas Cu_5O_3 binds it more weakly (**Figure 4, Table 1**). Most of the isomers feature the interaction of the C-C double bond of cyclohexene with Cu. This difference in binding energy may be explained in part by the coordination of the metal site to the C atoms of the C-C double bond. The order of adsorption strength also corresponds to average length of metal-carbon bonds such that Cu-C is ~2.0-2.1 Å in Cu_5O_5 (stronger adsorption); Pd-C is ~ 2.2 Å; Cu-C is ~2.1-2.9 Å in Cu_5O_3 (weaker adsorption). Moreover, Cu clusters rearrange considerably upon binding cyclohexene, exhibiting more open geometries, containing both O atoms at the cluster-surface interface and O atoms binding on top of the clusters. The average Cu-Cu bond length increases following binding of cyclohexene, ranging from 2.6-2.8 Å depending on the isomer. In contrast, average Cu-Cu bond lengths without the adsorbate and following cyclohexane adsorption remain at 2.6 Å. However, in rare configurations such as iii for Cu_5O_3 (**Figure 4**), cyclohexene is bound to the O atom in the cluster, with the C-O bond length being ~1.4 Å, close to the experimentally observed C-O bond of ~1.2 Å in cyclohexanone. Indeed, cyclohexanone is observed in the experiment as one of the products on Cu catalysts (**Figure 2**). This minimum also displays greater charge transfer from the cluster to cyclohexene of 0.22 e^-. Typically, charge transfer from the hydrocarbon to the Pd-O or Cu-O cluster is negligible, ranging from -0.1 to 0.1 e (**Tables S2-S15**).

Importantly, the ensemble of catalyst states transforms completely from the state with bound cyclohexane to the state with bound cyclohexene. In fact, considering the Cu-O cluster core, none of the low-energy species with cyclohexane can be linked to those with cyclohexene through a direct gradient-following relaxation. Hence, based on our model, we expect full catalyst reorganization as the reaction progresses, again leading to intermediate stabilization, competing with Pd-O. Hence, we see that catalyst isomerization (beyond just a relaxation) is part of the reaction coordinate. This observation exposes an intriguing fundamental question: does the system have enough time to fully dynamically rearrange in every reaction intermediate? Or does it not and instead follows a path connecting metastable states all the way

through the catalytic process? Or is the relaxation of the ensemble only partial? It is highly non-trivial to elucidate this dynamic aspect of cluster catalysis. We hope to provide some insight in forthcoming publications. In this work, we assume that all thermally-accessible geometric states are also kinetically accessible,[12] and that the time is sufficient for the full ensemble equilibration in every reaction intermediate. In fact, a reaction profile computed starting from the global minimum of adsorbate-free Cu_5O_3 or Cu_5O_5, and not considering the possibility of cluster isomerization, would be unfeasibly high in energy, not compatible with the experimentally-observed high reactivity on Cu-O, and not comparable with Pd-O. This serves as a partial support for our approach, and suggests that the standard view on the catalytic reaction profile that does not include thermal catalyst reorganization is likely generally incomplete, and thus calculated energetics may be misleading.

Previously proposed mechanisms for the ODH of cyclohexane to hydrocarbon products such as cyclohexene, cyclohexadiene, and benzene occur via dehydrogenation in a step-wise fashion (intermediate hydrocarbons formed through sequential C-C/C-H bond breaking) or direct dehydrogenation to benzene.[47,48] In zeolites, the presence of the Cu^{2+} oxidation state has been linked to adsorption of oxygen as the rate limiting step, leading to increased production of benzene.[49,50] Mochida, et. al. noted that in their pulse gas chromatographic techniques, pre-adsorbed O_2 pulsed with cyclohexane resulted in benzene but the reverse, pre-adsorbed cyclohexane pulsed with O_2, resulted in CO_2.[50] In our theoretical study, we focus on sequential dehydrogenation and the selectivity of the first dehydrogenation step: the ensemble-averaged ΔE_1 describing $C_6H_{12} \rightarrow C_6H_{10} + H_2$ on Pd_4O_2, Cu_5O_5, and Cu_5O_3 is shown in **Figure 5**. The affinity of the catalyst ensemble to cyclohexene is the lowest for Cu_5O_3 and stronger for Cu_5O_5 and Pd_4O_2. This suggests the higher likelihood of cyclohexene desorption from the Cu_5O_3 catalyst, as compared to other clusters, supporting experimentally observed selectivity. Thus, we can infer that the selectivity of ODH is due primarily to the secondary oxidation state of Cu present at 300°C, represented by the Cu_5O_3 clusters (**Figure 4**).

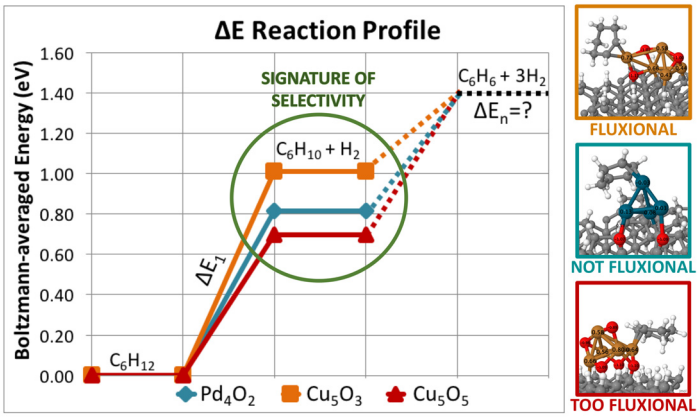

Figure 5. Boltzmann-averaged energetics illustrate the greater selectivity of supported Cu-O over Pd-O clusters for the first step of dehydrogenation, ΔE_1, for cyclohexane to cyclohexene.

Again, cyclohexene binding to Cu-O clusters with appreciable affinity results from strong geometric rearrangements of clusters, unique to small cluster sizes (but not characteristic of

Pd_4). Consequently, the reaction is facilitated by cluster fluxionality and dynamics, resulting in special selectivity. Our calculations reveal a great difference in binding energies to cyclohexene (0.32 eV) between Cu_5O_5 (-1.39 eV) and Cu_5O_3 (-1.07 eV). For the dominant structures in both cases, we computed the energy cost for the rearrangement of clusters upon adsorption as the difference between the frozen cluster geometry with removed adsorbate and the nearest relaxed minimum. For Cu_5O_3 the cluster rearrangement corresponds to the 0.81 eV energy-cost. For Cu_5O_5 it is 0.93 eV. Thus, the difference between them is ~ 40% of the binding energy difference. The remaining difference comes from the cluster isomerization beyond relaxation. This result suggests that Cu_5O_5 clusters are more flexible, stabilizing the bound reaction intermediate more and potentially resulting in activity that is less selective than that of Cu_5O_3. Hence, cluster dynamics and moderate fluxionality defines Cu_5O_3's greater selectivity, enabling a higher energetic step in dehydrogenation. At the electronic level, Cu atoms in Cu_5O_3 have less of a positive charge as compared to those in Cu_5O_5 (**Tables S9-S10**), suggesting that the electronic states responsible for binding and activating cyclohexene must align less well with cyclohexene's orbitals. Overall, both redox and geometric flexibility/fluxionality of Cu clusters in reaction conditions appears to be critical for the activity and selectivity of Cu catalysts. Clusters have to reduce first, and then access new, more stable geometries upon reagent binding, before being able to exhibit the observed selectivity. Flexibility also differentiates Cu clusters from Pd, in this way apparently making Cu clusters more "noble" or Pd-like at the electronic level, and catalytic toward ODH.

In this work we focus on the case of oxygen-deficient conditions, where C-H activation is known to be the rate-determining event. Undoubtedly, oxygen does play a role in ODH, but for the given conditions, the insight provided so-far appears satisfying. The role of oxygen in ODH, $C_6H_{12} + ½O_2 \rightarrow C_6H_{10} + H_2O$, is far from trivial to elucidate for such complex and dynamic catalysts as Cu-O clusters. While a previous study on supported-clusters explored the reaction profile by including $½O_2$, the direct participation via adsorption of O_2 on the cluster or hydrocarbon was not pursued.[50] In other surface-mediated reactions, the dynamics of pressure-dependent O_2 may lead to increased production of CO_2,[47] but in other systems where the oxidative state of Cu is of interest, the presence of O_2 followed by introduction of cyclohexane has led to greater production of benzene while the reverse led to CO_2.[49,50] These experimental studies merely reinforce the complexity of O_2's presence and likewise our theoretical calculations uncover a range of interactions. The affinity and placement of O_2 on the clusters is isomer-dependent. Moreover, oxygen in the cluster or gas phase O_2 may participate in the reaction, potentially coinciding with the evolution of the cluster oxidation state during reaction conditions. We attempted to further explore the interaction between O_2 and Cu-catalysts with bound cyclohexane, and some results are presented in the **Table 1** and **SI** (**Figures S17, S18**, **Tables S11-S13**). We witness a variety of events, such as the further cluster oxidation, spontaneous C-H scission, production of alcohols, hydroxylation on the support, all of which are Cu-O isomer dependent. It is clear the mechanistic possibilities are numerous and diverse. However, our limited exploration of O_2 adsorbed on the four lowest minima of Cu_5O_5-C_6H_{12} and Cu_5O_3-C_6H_{12} at first dehydrogenation step with O_2 ($C_6H_{12} + ½O_2 \rightarrow C_6H_{10} + H_2O$) does support the trend of Cu_5O_5 being less selective than Cu_5O_3.

We invite the reader to notice the complexity of the involved reaction profiles that begins to transpire for the studied reaction. Given so many structurally different states of the system in the reactant state and the reaction intermediate, unclear ways in which these states connect to each other in the swarm of the reaction profiles, as well as the multitude of unique ways in

which the reaction might involve oxygen (i.e. atoms coming from the gas phase O_2 approaching in a variety of ways, or from the oxidized clusters), the number of possibilities for the mechanism is inconceivably large. We recognize that not reporting at least one full reaction profile looks like a step back from what has been known in the catalysis literature for a while. However, the real complexity of the dynamic interface that we unravel is a relatively new phenomenon, which was never addressed in the studies reporting full reaction mechanisms. There is no way all the mechanistic possibilities could be explored for such a dynamic interface as we see here. And thus, it is impossible to single out one or even a few of these mechanisms that could be dominant. Such an exploration is way beyond our capabilities right now.

Summary

We report two classes of highly active catalysts, oxidized Pd and Cu clusters, for the ODH of cyclohexane, with distinctly different selectivity towards C6 products: Pd primarily produces benzene, while Cu displays the highest selectivity towards desirable cyclohexene. The support- and size-dependent performance of the Pd clusters illustrates ways of tuning the performance of the catalyst, whereas Cu clusters highlight the considerable effect of the metal's oxidation state on activity and/or selectivity. Theoretical results are in accordance with the experimental findings and underline the importance of understanding the nature of the active site under reaction conditions. The oxidation state and the differences in fluxionality of cluster catalyst ensembles determine selectivity; hence, cluster geometric and redox flexibility are tunable knobs in cluster catalysis design. Our observations underline the importance of finding the catalytically-relevant ensemble of catalyst states that develop during reaction conditions, particularly in the selectivity-determining intermediate.

Experimental Methods

Catalyst preparation and *in situ* characterization. The supports were prepared by depositing ~3 monolayer Al_2O_3, and ~1 nm TiO_2 on a naturally oxidized P-doped Si(100) substrate in a custom viscous flow ALD reactor.[7,46] The oxide layer thickness determined by ellipsometry is ~0.7 nm. UNCD supports (~250 nm thick, on a Si(100) chip) were purchased from Advanced Diamond Technologies (UNCD, 25 Aqua DoSi). The clusters are produced in a liquid nitrogen cooled magnetron condensation source at high vacuum. The beam of clusters cations is guided towards the substrate. Cluster size–selection occurs at a quadrupole mass filter prior to deposition. The impact energy of the landing clusters is kept below 1eV/ atom by applying a retarding potential to the support.[32] After deposition, the as made metallic cluster samples are exposed to air, which typically leads to their oxidation/hydroxylation There was no reduction or oxidation step applied prior the *in situ* experiments. The *in situ* TPRx, combined with GISAXS, and GIXANES in fluorescence mode are performed using a reaction cell of ~20 cm^3 internal volume. The catalyst samples are placed on a ceramic surface heater with temperature (T) controlled using a K-type thermocouple attached to a T controller with a precision <+-0.5ºC. A slow heating rate (10ºC/ min; see **Figure 1a** for the T-ramp) is used in order to attain equilibrium. Data is collected over 25 minutes at each T. The reactant mixture used was 0.4 % cyclohexane and 4 % O_2 seeded in He, fed to the reaction cell at a flow rate of 20 sccm.

Theoretical methods. We performed PW-DFT calculations with VASP, using the PBE+D3, with kinetic energy cut-off of 400 eV (see SI for Refs.). The (100) surface was

modeled as a (4x4) slab and >14 Å of separating vacuum layer. The convergence criteria were 10^{-6} (10^{-5}) eV for electronic (geometric) relaxations. A 2x2x1 Monkhorst-Pack k-point grid was utilized for all calculations. The bottom 2 layers were fixed. Terminal hydrogens were added to the top and bottom of the slab. Adsorption energies were calculated as E_{reag}(ev) = E [surf + M-O + E_{reag}] – E [surf + M-O_{glob}] – $E_{gas,reag}$. To gauge selectivity of supported clusters for cyclohexane to benzene formation, we concentrated on the first dehydrogenation step ($C_6H_{12} \rightarrow C_6H_{10}+H_2$) for the ensemble-average:

$\mathbf{\Delta E}_{C6H12->C6H10+H2}$ (ev) = ($\mathbf{\Sigma} P_{535K} E_{tot}$ [surf + M-O + E_{C6H10}] + E_{gas} [H_2]) – E [surf + M-O_{min} + E_{C6H12}]

where P_{535K} is the Boltzmann probability for *i*-th configuration.

Acknowledgements

The work at Argonne (A.H., B.Y., M.J.P., S.V.) was supported by the US Department of Energy, BES Materials Sciences under Contract DEAC02–06CH11357 with UChicago Argonne, LLC, operator of Argonne National Laboratory, the work at the Advance Photon Source (beamline 12-ID-C, S.S.) by the US DOE, Scientific User Facilities under Contract DEAC02-06CH11357. A.N.A. thanks AFOSR grant FA9550-16-1-0141. The sampling algorithm development by H.Z. was sponsored by the US DOE-BES DE-SC0019152 grant to A.N.A. CPU resources at the DoD High Performance Computing Modernization Program (AFRL DSRC, ERDC, and Navy DSRC), supported by the DOD, and XSEDE were used. M.-A.H. thanks the UCLA Dissertation Fellowship. S.V. also acknowledges support from the European Union's Horizon 2020 research and innovation programme under grant agreement No 810310, which corresponds to the J. Heyrovsky Chair project ("ERA Chair at J. Heyrovský Institute of Physical Chemistry AS CR – The institutional approach towards ERA") during the finalization of the paper. The funders had no role in the preparation of the article.

Keywords: cluster dynamics, cyclohexane oxidative dehydrogenation, deposited clusters, selectivity control, size-selected subnanometer clusters

References

1. E. C. Tyo, S. Vajda, , *Nat. Nanotechnol.* **2015,** *10*, 577-588.
2. S. Vajda, M. J. Pellin, J. P. Greeley, C. L. Marshall, L. A. Curtiss, G. A. Ballentine, J. W. Elam, S. Catillon-Mucherie, P. C. Redfern, F. Mehmood, P. Zapol, *Nat. Mater.* **2009,** *8*, 213-216.
3. S. Vajda, M. G. White, *ACS Catal.* **2015,** *5*, 7152-7176.
4. Z. Luo, A. W. Castleman, Khanna, S. N., *Chem. Rev.* **2016,** *116*, 14456-14492.
5. Y. Lei, F. Mehmood, S. Lee, J. Greeley, B. Lee, S. Seifert, R. E. Winans, J. W. Elam, R. J. Meyer, P. C. Redfern, D. Teschner, R. Schlögl, M. J. Pellin, L. A. Curtiss, S.Vajda, *Science* **2010,** *328*, 224-228.
6. E. Jimenez-Izal, A. N. Alexandrova, *Ann. Rev. Phys. Chem.* **2018**, *69*, 377-400.
8. W. E. Kaden, T. Wu, W. A. Kunkel, S. L. Anderson, *Science* **2009**, *326*, 826-829.
9. U. Heiz, F. Vanolli, A. Sanchez, W. D. Schneider, *J. Am. Chem. Soc.* **1998**, *120*, 9668–9671.
10. E. T. Baxter, M.-A. Ha, A. C. Cass, A. N. Alexandrova, S. L. Anderson, *ACS Catal.* **2017,** *7*, 3322-3335.

11. M.-A. Ha, E. T. Baxter, A. C. Cass, S. L. Anderson, A. N. Alexandrova, *J. Am. Chem. Soc.* **2017,** *139*, 11568-11575.
12. H. Zhai, A. N. Alexandrova, **2018,** *9*, 1696-1702.
13. E. Jimenez-Izal, J.-Y. Liu, A. N. Alexandrova, *ACS Catal.* **2018**, *8*, 8346-8356.
14. H. Zhai, A. N. Alexandrova, , *J. Chem. Theor. Comput.* **2016,** *12* (12), 6213-6226.
15. E. Jimenez-Izal, J.-Y. Liu, A. N. Alexandrova, *J. Catal*. **2019**, *under revision.*
16. M.-A. Ha, J. Dadras, A. N. Alexandrova, *ACS Catal.,* **2014**, *4*, 3570-3580.
17. J. Dadras, L. Shen, A. N. Alexandrova, *J. Phys. Chem. C,* **2015**, *119,* 6047-6055.
18. S. Matar, *Chemistry of Petrochemical Processes*. Gulf Professional Publishing, Oxford: 2001.
19. H. H. Kung, *Advances in Catalysis*. Academic Press: 1995; Vol. 40.
20. B. Sarkar, C. Pendem, L. N. S. Konathala, T. Sasaki, R. Bal, , *Catal. Comm.* **2014,** *56*, 5-10.
21. E. C. Tyo, C. R. Yin, M. Di Vece, Q. Qian, G. Kwon, S. Lee, B. Lee, J. E. DeBartolo, S. Seifert, R. E. Winans, R. Si, B. Ricks, S. Goergen, M. Rutter, B. Zugic, M. Flytzani-Stephanopoulos, Z. W.Wang, R. E. Palmer, M.Neurock, S. Vajda, , *ACS Catalysis* **2012,** *2*, 2409-2423.
22. M. Panizza, C. Resini, G. Busca, E. Fernández López, V. Sánchez Escribano, *Catal. Lett.* **2003,** *89*, 199-205.
23. E. C. Alyea, M. A.Keane, *J. Catal.* **1996,** *164*, 28-35.
24. K. Sato, M. Aoki, R. Noyori, *Science* **1998,** *281* (5383), 1646-1647.
25. K. Weissermel, H.-J. Arpe, *Industrial Organic Chemistry*. 4th ed.; Wiley‐VCH Verlag GmbH & Co. KGaA: 2003.
26. J. C. Walton, A. Studer, *Acc. Chem. Res.* **2005,** *38* (10), 794-802.
27. H. M. AbdelDayem, M. Faiz, H. S. Abdel-Samad, S. A. Hassan, *J. Rare Earths* **2015,** *33*, 611-618.
28. Y. Liu, H. Tsunoyama, T. Akita, S. Xie, T. Tsukuda, *ACS Catalysis* **2011,** *1* (1), 2-6.
29. N. F. Dummer, S. Bawaked, J. Hayward, R. Jenkins, G. J. Hutchings, *Cat. Today* **2011,** *160* (1), 50-54.
30. B. Coughlan, M. A. Keane, *Catal. Lett.* **1990,** *4* (3), 223-233.
31. S. L. Nauert, F. Schax, C. Limberg, J. M. Notestein, *J. Catal.* **2016,** *341*, 180-190.
32. C. Yin, E. Tyo, K. Kuchta, B. von Issendorff, S. Vajda, , *J. Chem. Phys.* **2014,** *140*, 174201.
33. M. Jin, P. Lu, G. X. Yu, Z. M. Cheng, L. F. Chen, J. A. Wang, *Catal. Today* **2013,** *212*, 142-148.
34. Y. J. Zhu, J. Li, X. G. Yang, Y. Wu, *Chem. Let.* **2004,** *33*, 822-823.
35. M. Lezanska, G. S. Szymanski, P. Pietrzyk, Z. Sojka, J. A. Lercher, , *J. Phys. Chem. C* **2007,** *111*, 1830-1839.
36. H. I. Zhu, Q. J. Ge, W. Z. Li, X. B. Liu, Xu, Y. H., *Catal. Lett.* **2005,** *105* (1-2), 29-33.
37. M. C. Kung, H. H. Kung, *J. Catal.* **1991,** *128* (1), 287-291.
38. J. N. Guo, J. Z. Lin, X. Liu, Q. W. Wang, G. Gao, X. Zhang, X. G. Shi, B. Yang, H. B. Jin, *Adv. Mat. Res.* **2014,** *953-954*, 1261-1268.
39. Chen, Y.; Vlachos, D. G. *J. Phys. Chem. C* **2010**, *114*, 4973−4982.
40. H. Zhai, A. N. Alexandrova, *ACS Catal.* **2017**, *7*, 1905–1911.
41. G. Sun, P. Sautet, *J. Am. Chem. Soc.* **2018**, *140*, 2812–2820.
42. A. Walch, A. A. Sokol, J. Buckeridge, D. O. Scanlon, R. A. Catlow, „*J. Phys. Chem. Lett.* **2017**, *8*, 2074–2075.

43. J. De Roche, C. M. Gordon, C. T. Imre, M. D. Ingram, A. R. Kennedy, F. L. Celso, A. Triolo, *Chem. Mater.* **2014**, *26*, 3089–3097
44. Z. Zhang, E. Jimenez-Izal, I. Hermans, A. N. Alexandrova, *J. Phys. Chem. Lett.* **2019**, *10*, 20-25.
45. B. Zandkarimi, A. N. Alexandrova, *J. Phys. Chem. Lett.* **2019**, *10*, 460-467.
46. H. Feng, J. W. Elam, J. A. Libera, M. J. Pellin, P. C. Stair, *J. Catal.* **2010,** *269*, 421-431.
47. E. C. Alyea, M. A. T. Keane, *J. Catal.* **1996,** 164, 28-35.
~~48. H. Feng, J. W. Elam, J. A. Libera, M. J. Pellin, P. C. Stair, *J. Catal.* **2010**, 269, 421-431.~~
48. B. Coughlan, M. A., Keane, *Catal. Lett.* **1990**, *4*, 223-233.
49. I. Mochida, T. Jitsumatsu, A. Kato, T. Sciyama, *J. Catal.* **1975**, *36*, 361-370.
50. S. Lee, A. Halder, G. A. Ferguson, S. Seifert, R. E. Winans, D. Teschner, R. Schlögl, V. Papaefthimiou, J. Greeley, L. A. Curtiss, S. Vajda, *Nat. Comm.* **2019**, *10*, 954.

TOC Graphics:

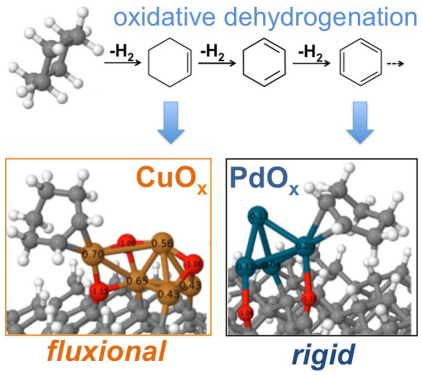

"Cluster catalysts for oxidative dehydrogenation of cycloxehane with highly-competitive activity and extraordinary selectivity controlled by cluster dynamics under reaction conditions are reported.